Available at www.sciencedirect.com

ScienceDirect

journal homepage: www.elsevier.com/locate/issn/15375110

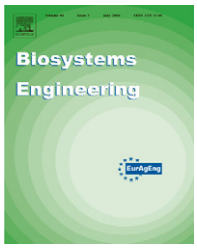

Research Paper: PM—Power and Machinery

Anchor mechanism to increase the operator clearance zone on narrow-track wheeled agricultural tractors: Static and field upset test results

H. Silleli[a,*], M.A. Dayıoğlu[a], A. Gültekin[b], G. Saranlı[b], M.A. Yıldız[b], E. Akay[b], K. Ekmekçi[c]

[a]Department of Farm Machinery, Agricultural Faculty of Ankara University, 06130 Aydinlikevler, Ankara, Turkey
[b]Turk Traktor and Ziraat Makineleri A.S. Guvercinyolu, 111-112, 06041 Gazi, Ankara, Turkey
[c]Ministry of Agriculture and Rural Affairs, Directorate of Agricultural Equipment and Machinery Test Centre, P.O. Box 96, 06172 Yenimahalle, Ankara, Turkey

ARTICLE INFO

Article history:
Received 26 September 2007
Received in revised form
18 October 2007
Accepted 22 October 2007
Available online 21 December 2007

In agricultural activities, tractor overturning remains a serious problem. As an additional system to rollover protective structures (ROPS) for reducing the risk of overturning, anchor mechanisms can provide an increased safety zone for the driver. In this study, the effectiveness of an anchor mechanism for narrow-track agricultural tractors was examined. To determine the strength of the system, a static side-loading test and field test were performed to the anchor mechanism. In the field test, strain gauges were installed to determine the forces affecting the anchor mechanism. In order to interpret the overturning behaviour, accelerometers and orientation sensors were attached on to the tractor. During the test, the tractor rolled over up to 119°. According to the video images, the time between the front tyre coming off the ground and the anchor hitting the ground was 520 ms while the total time of overturning was 720 ms.

© 2007 IAgrE. Published by Elsevier Ltd. All rights reserved.

1. Introduction

Tractor overturning accidents remain a serious problem within the agricultural industry, and need to be reduced (Liu & Ayers, 1998). Tractor overturning not only causes injuries and fatalities; it also results in machine damage and loss of productive time (Murphy & Sommer, 2004). In many industrialised countries, tractors cause 15–45% of work-related fatalities among those employed in agriculture. In order to reduce tractor-related deaths and serious injuries, studies are continuing to develop standards and regulations; to apply new technology and design solutions; to promote of ROPS; and to develop alternative designs (Day *et al.*, 2005). To characterise their new design of the spring-operated telescopic system, Etherton *et al.* (2002) performed both static laboratory experiments which complied with the ASAE J2194 standards and field upset tests. Their static tests were conducted to determine the design parameters of the system when the system was fully opened and in the locked position. Silleli *et al.* (2007) introduced an additional system for narrow-track orchard and vineyard tractors. The system increased the protection efficiency of the ROPS for the tractor operators and at the same time reduced the overhead clearance required by these machines in order to improve potential usage in orchard and vineyard conditions.

Current standards require that a ROPS must protect the tractor operator from injury when the tractor undergoes a

*Corresponding author.
E-mail addresses: hsilleli@agri.ankara.edu.tr (H. Silleli), ayding@turktraktor.com.tr (A. Gültekin), kekmekci@tamtest.gov.tr (K. Ekmekçi).
1537-5110/$ - see front matter © 2007 IAgrE. Published by Elsevier Ltd. All rights reserved.
doi:10.1016/j.biosystemseng.2007.10.014

Nomenclature

A	area of the anchor, mm^2
B	minimum outer width of the tractor, m
B_6	width of the protective structure between the right and left points of impact, m
d	diameter of the anchor, mm
E	modulus of elasticity, $N\,mm^{-2}$
E_{is}	absorbed energy by the protective structure, kJ
F_x	impact load in the x direction, N
F_y	impact load in the y direction, N
F_z	impact load in the z direction, N
εF_x	strain due to the load F_x, με
εF_y	strain due to the load F_y, με
εF_z	strain due to the load F_z, με
L	length of the anchor, mm
M	the tractor mass, t
εS_1	strain for S_1 strain gauge, με
εS_2	strain for S_2 strain gauge, με
εS_3	strain for S_3 strain gauge, με

single overturn. During an overturn the operator should occupy a "critical zone" that should be protected from entering by any part of the tractor, the ground or by the ROPS (Myers, 2000). This critical zone named in the OECD Codes published in 2007 as a "clearance zone" is defined according to the vertical plane, generally longitudinal to the tractor, and passes through the Seat Reference Point (SRP) and the centre of the steering wheel. Normally this vertical reference plane coincides with the median plane of the tractor and it tends to move horizontally with the seat and the steering wheel during the test, but to remain perpendicular to the tractor or the floor of the protective structure. During the test it is controlled with a clearance zone apparatus, which has constant dimensions representing the tractor driver who is in the overturning accident.

Accidents resulting from tractor overturns on slopping ground arise from a lack of stability or control loss (Spencer *et al.*, 1985). In order to analyse tractor behaviour during an overturn, stability factors should be determined. Liu and Ayers (1998) classified the stability of a tractor into static and dynamic. They explained that the reasons for static stability are the dimensions and the centre of gravity of a tractor, but emphasised that dynamic stability is a more complex and a more realistic assessment of tractor stability. They also mentioned that the pitch and roll angles can be used as an input to calculate the position of a vehicle and to develop a criterion of stability.

The objective of this research is to determine the strength of the anchor mechanism by using a static side-loading test and a field test. In the field test, strain gauges were installed on both the anchor mechanism and ROPS during rollover. The dynamic behaviour of the tractor during overturning was determined by measuring the turning angle, angular velocities and accelerations *versus* time.

2. Materials and methods

2.1. Static side-loading test

A static side-loading test was performed in the laboratory to test the ROPS which has already been approved by the OECD Code 6 (OECD, 2007; OECD Code 6, 2007). The test was conducted in an authorised station for testing ROPS according to the OECD Codes in the Ministry of Agriculture and Rural Affairs, Directorate of Agricultural Equipment and Machinery Test Centre, Turkey. In order to determine the strength of the anchor and chase and the locking pins, static testing was only performed on the anchor in accordance with the side-loading procedure of OECD Code 6. The load was applied normal to the cross section of the anchor while it was fully open in its locked position.

The ROPS was formed from a steel tube of 48 mm outside diameter with a wall thickness of 7 mm and it was strengthened by use of a 32 mm steel circular bar inserted into the tube at the base. For the anchor housing an Fe360C steel tube was used; the diameter of the tube was determined to be 73 mm with a wall thickness of 6 mm. The Fe510D steel bar was used for the anchor and its outside diameter was selected as 48 mm. The anchor mechanism was also accompanied by latch pins, which lock and prevent the anchor from closing after deployment during rollover. The anchor mechanism can be seen in Fig. 1.

A static loading test was performed via a Visual BASIC program and PC link under displacement and load control. The loading rate was at $5\,mm\,s^{-1}$ throughout the test. The program constantly computed the total energy applied based on the area under the force–deflection data. Loading was provided by a hydraulic actuator with a capacity of 250 kN. In the test, the load application point was selected for the end of the anchor, which is likely to hit the ground first in a sideways

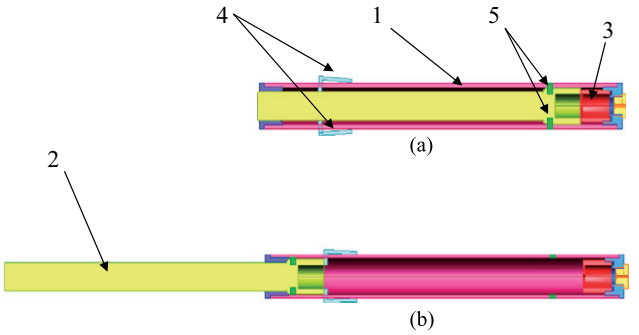

Fig. 1 – Principle of release and lock mechanism of the anchor mechanism: (a) cross-section of closed position of the anchor ready to be deployed; (b) cross-section of the anchor mechanism after deploying; (1) housing of the anchor mechanism; (2) anchor; (3) cartridge; (4) latch pins; (5) safe pins (Silleli *et al.*, 2007).

overturning accident. According to the SRP coordinates, the clearance zone apparatus was located as the place for referring the driver position in the event of an overturning. The energy absorbed by the protective structure during the test was calculated as established in the OECD Code 6 as

$$E_{is} = 1.75M(B_6 + B)/2B, \quad (1)$$

where E_{is} is the absorbed energy by the protective structure in kJ; M is the tractor mass in tones; and B_6 is the width of the protective structure between the right and left points of impact in m; and B is the minimum outer width of the tractor in m.

Table 1 – The specifications of data logger and strain gauges and accelerometer

Data logger	eDAQ Plus (Somat-nCode, USA)
Strain gauge measurement channel	8 channel low-level board
Accelerometer measurement channel	16 channel high-level board
Strain gauge supply voltage	10 V bipolar
Rosette strain gauge	CEA-06-125UR-350 (Vishay Measurement Group, USA)
Nominal gauge factor	2.12
Single-axle strain gauge	CEA-06-125UN-350 (Vishay Measurement Group, USA)
Nominal gauge factor	2.1
Accelerometer	CXL10LP3 (±10 g) (Crossbow Technology Inc., USA)
Accelerometer sensitivity	0.201 V g^{-1}
Sampling rate	2500 Hz
Data logging software	TcE 1.4.3 (Somat-nCode, USA)
Data processing software	Ice-Flow 3.0 Glypworks (Somat-nCode, USA)

2.2. *Field upset test*

A field-overturning test was carried out. The inclination of the field was shaped as required in ASAE J2194 (ASAE, 2002). The tests were performed by use of a radio-controlled full-size tractor, equipped with a measuring system. The main aim of these experiments was to determine the force values that the anchor has been exposed to throughout the course of the dynamic tests. In order to determine the loads in three axes individually, single strain gauges at three different directions had been stuck on the anchor. A rosette gauge was installed on the critical location of the ROPS determined by the ANSYS analysis to find out the effects of the anchor mechanism on the current ROPS design.

The single gauges were used to determine the forces whereas the rosette gauges were used for calculating the principle strains. Besides the strain gauges, a three-dimensional (3D) accelerometer and a gyroscope were used to determine the overturning angle and the duration of overturning time. The behaviour of the tractor during rollover was recorded with two digital video cameras placed at different viewpoints. During the test, the tractor was equipped with a data logger (eDAQ; Somat-nCode, USA), a 3D accelerometer and an MTi (Xsens Technologies B.V.) orientation sensor. The Somat-nCode eDAQ modular data acquisition system and the specifications for the strain gauges and accelerometer are given in Table 1.

The orientation sensor MTi is used as a complete inertial measurement unit with an integrated 3D magnetometer (3D compass), an embedded processor capable of calculating roll, pitch and yaw in real time, as well as outputting calibrated 3D linear acceleration, rate of turn (gyro) and (earth) magnetic field data. The performance specifications of the MTi sensor are given in Table 2. In order to determine the position of the tractor and to decide the overturning time during field testing, the roll, pitch and yaw angle should be considered. The directions of these parameters that were accepted for determining the tractor motion can be seen in Fig. 2.

Table 2 – The performance specifications of the orientation sensor MTi

	Rate of turn	Acceleration	Magnetic field
Unit	rad s^{-1}	m s^{-2}	mGauss
Dimensions	3	3	3
Linearity (% of full scale)	0.1	0.2	1
Bias stability (compensated)	5	0.02	0.5
(Uncompensated)	1	0.02	–
Scale factor stability (compensated)	–	0.05	0.5
(Uncompensated)	0.15	0.03	0.5
Noise (unit RMS)	0.7	0.01	4.5
Alignment error (°)	0.1	0.1	0.1
Bandwidth (Hz)	50	30	10
Physical structure	MEMS solid state, monolithic, beam structure, capacitative readout	MEMS solid state, capacitative readout	Thin film magnetoresistive

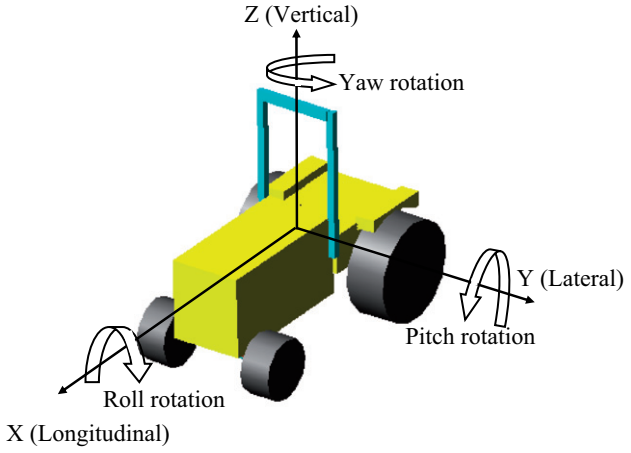

Fig. 2 – Definition of the directional axis describing tractor motion in three dimensions.

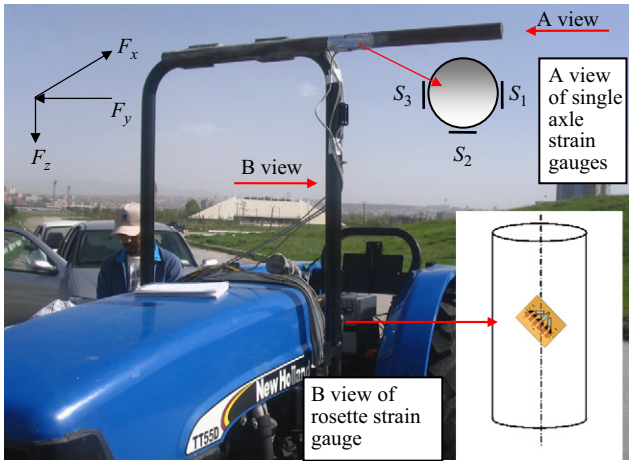

Fig. 3 – Installation of single-axle strain gauges and rosette strain gauge.

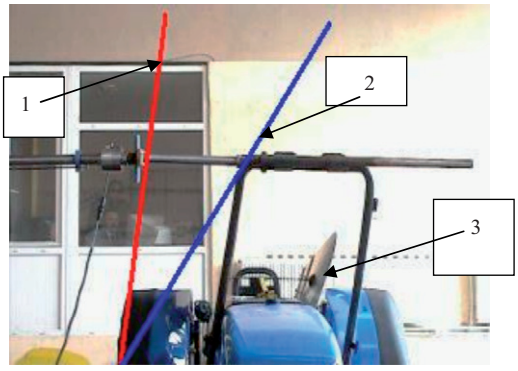

Fig. 4 – The comparison of the static loading test for the anchor mechanism and the rollover protective structure without an anchor at the moment of the maximum loading position of the test: (1) simulated ground plane for the anchor mechanism; (2) simulated ground plane for the rollover protective structure; (3) apparatus of clearance zone.

The installation of three single-axis strain gauges and a rosette strain gauge is shown in Fig. 3. Single strain gauges (S_1, S_2 and S_3) have been used for determining the three directional load values that were generated due to the forward speed of the tractor, overturning speed and twisting to the anchor. The relationships between the direction of the forces and measured strain values for three single gauges are represented by

$$\varepsilon S_1 = -\varepsilon F_x - \varepsilon F_y, \tag{2}$$

$$\varepsilon S_2 = -\varepsilon F_Y - \varepsilon F_z, \tag{3}$$

$$\varepsilon S_3 = \varepsilon F_x - \varepsilon F_y, \tag{4}$$

where εS_1 is the strain for S_1 strain gauge in με; εS_2 is the strain for S_2 strain gauge in με; εS_3 is the strain for S_3 strain gauge in με; εF_x is the strain due to the load F_x in με; εF_y is the strain due to the load F_y in με; and εF_z is the strain due to the load F_z in με. By combining Eqs. (2) and (4), the strain value εF_y can be calculated as shown below

$$\varepsilon F_y = -\tfrac{1}{2}(\varepsilon S_1 + \varepsilon S_3). \tag{5}$$

By inserting this value into Eq. (2), the εF_x value can be obtained as given below

$$\varepsilon F_x = -\tfrac{1}{2}(\varepsilon S_1 - \varepsilon S_3). \tag{6}$$

By combining Eqs. (3) and (5), the strain value represented by εF_z can be calculated as

$$\varepsilon F_z = -\tfrac{1}{2}(\varepsilon S_1 - 2\varepsilon S_2 + \varepsilon S_3). \tag{7}$$

Considering the loading conditions, the load generated on the y direction is perpendicular to the cross section of the anchor whereas the forces in the x and z directions impose bending moments on the bar. Consequently, the resulting forces can be calculated by use of

$$F_x = \frac{\pi}{32} EA \frac{d^3}{L} \varepsilon F_x, \tag{8}$$

$$F_y = EA\varepsilon F_y, \tag{9}$$

$$F_z = \frac{\pi}{32} EA \frac{d^3}{L} \varepsilon F_z, \tag{10}$$

where F_x is the impact load in the x direction in N; F_y is the impact load in the y direction in N; F_z is the impact load in the z direction in N; E is the modulus of elasticity in N mm^{-2}; d is the diameter of anchor in mm; L is the length of the anchor in mm; and A is the area of the anchor in mm^2.

3. Results and discussion

3.1. *Static side-loading test results*

The static tests were performed in accordance with the OECD Code 6 side-loading procedure. Fig. 4 shows the deflection while the maximum load is applied. After the test, no cracks or failures were observed on the anchor mechanism, ROPS, joints and latch pins. When the test results are compared in terms of the simulated ground planes, it is seen that while ROPS without the anchor came in close to the limits of the

zone of the clearance apparatus, in the presence of the anchor, the results were improved.

The static test result is given in Fig. 5. According to the test, the maximum load was found to be 22.54 kN and the maximum deflection attained was 195.9 mm. The plastic deformation was also found to be 68.3 mm. After the test, the maximum absorbed energy was calculated to be 2.81 kJ.

3.2. *Field upset test result*

Fig. 6 shows an image sequence captured during a side overturning while the tractor speed was 8.42 km h^{-1}. The overturning time was determined by a video capture programme, which had 40 ms capturing capability. According to the video images, the time between the front tyre leaving the ground and the anchor hitting the ground was 520 ms while the total time of overturning was 720 ms.

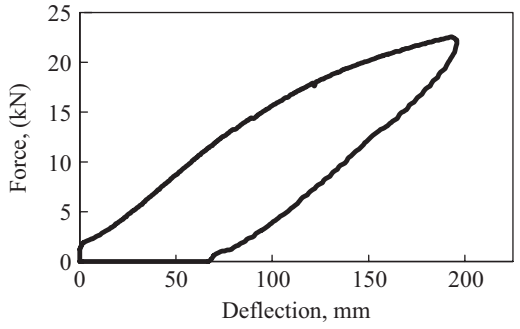

Fig. 5 – Force versus deflection graph of the static side-loading test result.

Fig. 7 presents the time history for the overturning angle obtained from the MTi sensor of the tractor. Roll, pitch and yaw angles can be seen on the curve. These curves provide the overturning duration and overturning angle in three directions. When the curve in Fig. 7 is closely examined the overturning started at 267 s and finished at 268 s. Considering the roll angle, it can be seen that initially the tractor rolled over up to 119° and then came back to 107.7° because it bounced due to the elasticity on the ROPS. Upon reaching the instability angle of 50.58°, the tractor began to roll and came to a stop at an angle of 119° within 750 ms. At the end of the overturning, it was found that the anchor had penetrated about 200 mm into the ground resulting in an extra 6° of overturn. It was also found that the ROPS had deformed permanently 8°. The tractor turned 14° due to penetration into the ground and plastic deformation. As a result, the anchor hit the ground at 95° during the rollover. Examining the pitch angle, it can be found that there is an 18° rotation in pitch direction upon completion of the rollover. The rotation around the rear tyre was caused by the anchor acting as a pivot for the tractor. A 60° change in yaw angle occurred due to the nature of the overturn, which occurred during the test.

The MTi orientation sensor was reliable and found to be accurate enough to use as a control sensor for the deployment system. In addition to the orientation sensor, an additional accelerometer was used to determine the overturning characteristics. As can be seen from Fig. 8, the

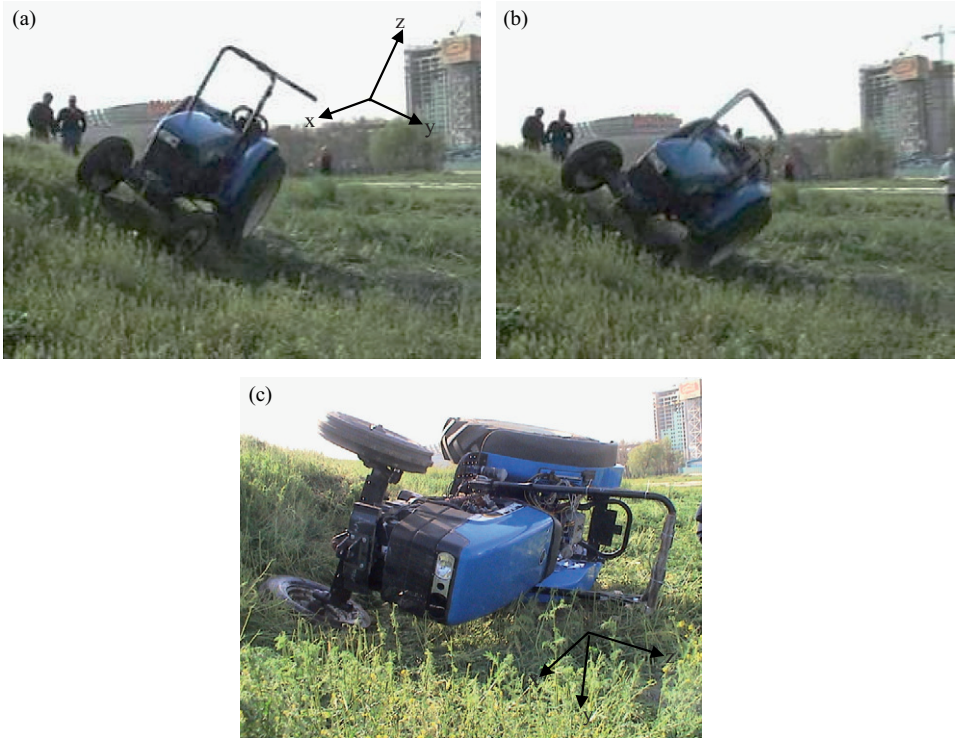

Fig. 6 – Field upset test with an anchor mechanism: (a) instability position; (b) the lifting of the front wheel; (c) overturned tractor.

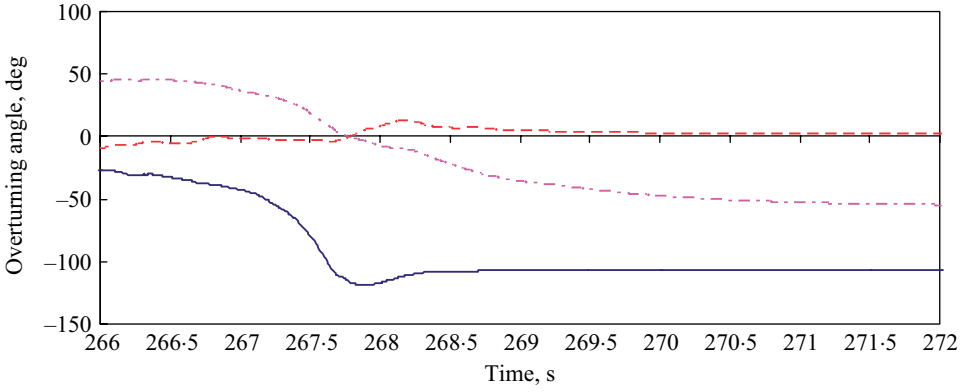

Fig. 7 – Overturning angle versus time graph: ——, roll angle; – – –, pitch angle; — · —, yaw angle.

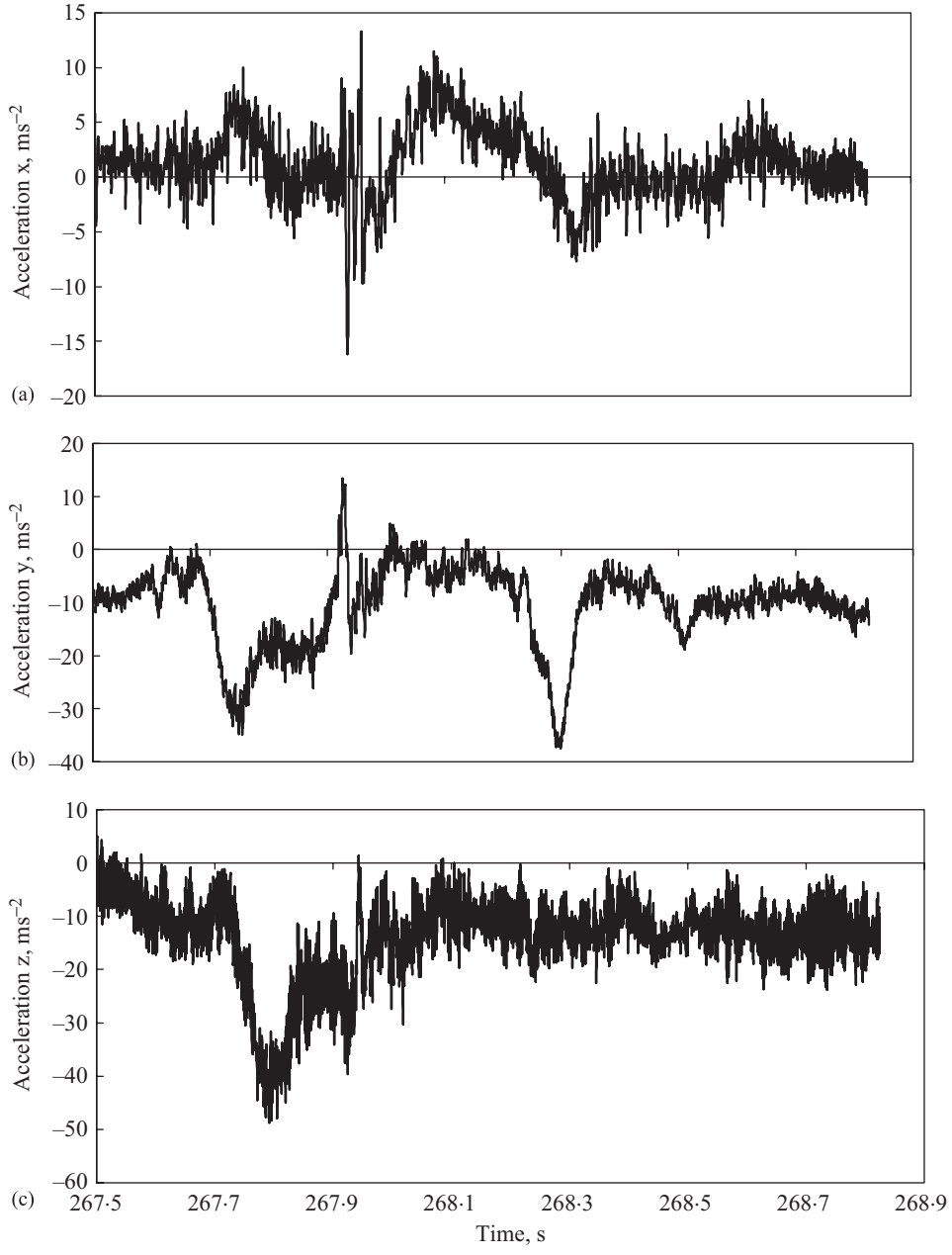

Fig. 8 – Time history data for acceleration in three directions: (a) acceleration in the *x* direction; (b) acceleration in the *y* direction; (c) acceleration in the *z* direction.

acceleration values in the z direction (z-direction considered at the overturned position) was found to be maximum when it was compared with the values for the other two directions.

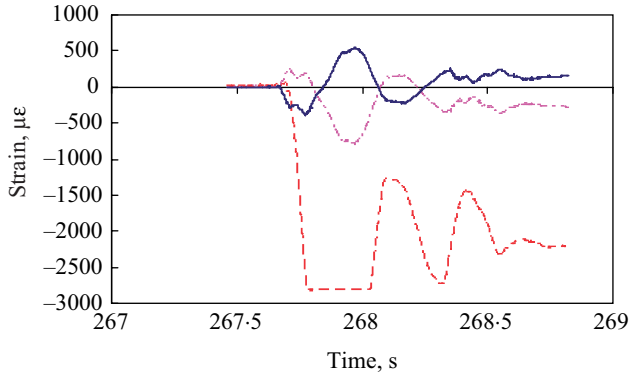

Fig. 9 – Strain versus time data for three single gauges installed on the anchor: ———, time history of the single axis strain gauge (S_1); – – –, time history of the single axis strain gage (S_2); — · —, time history of the single-axis strain gauge (S_3).

This value was determined at the 116° as $-48.74\,m\,s^{-2}$. The anchoring effect and the rolling direction of the tractor and inclination of the test field caused this value to be amplified. The three peak values for the y direction were measured as −34.79, 11.08 and $-37.11\,m\,s^{-2}$. It is suggested that the sinusoidal characteristics of the acceleration curve were due to the soil damping effects and elastic deformation of the ROPS. This can be interpreted from Fig. 7 when the change of the roll angle from 119° to 107.7° is considered. Additionally, plastic deformation was observed in this direction. The acceleration in the *x*-axis, representing the travelling direction of the tractor, was measured as $-15.62\,m\,s^{-2}$ at an inclination of 118°.

3.3. *Strain gauge results*

The strain values S_1, S_2 and S_3, which are measured by use of single gauges during the field test are given in Fig. 9. Due to gain settings, strain values higher than 2810 με could not be measured with the strain gauge S_2. However, this did not affect the calculation of the force values in the *x* and *y*

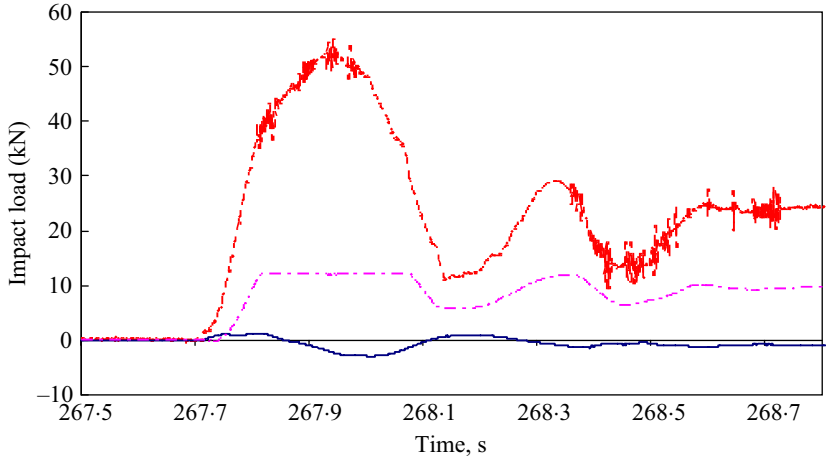

Fig. 10 – Impact load versus time data for field test at 8.42 km h^{-1}: ———, impact load (F_x); – – –, impact load (F_y); — · —, impact load (F_z).

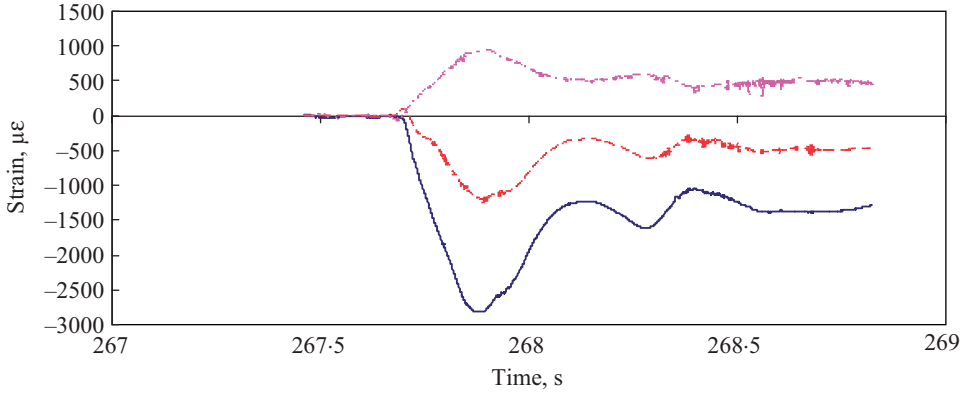

Fig. 11 – Strain versus time graphs for rosette gages for the field upset test: ———, time history of the rosette gage (R_1); – – –, time history of the rosette gage (R_2); — · —, time history of the rosette gage (R_3).

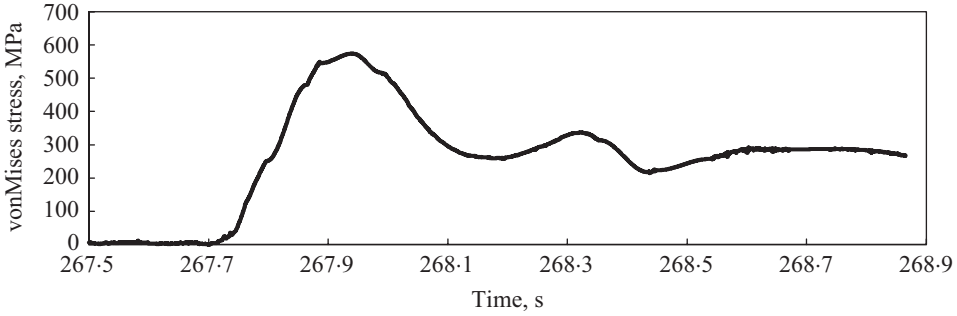

Fig. 12 – Stress versus time graphs for rosette gauges: max principal stress on the rollover protective structure.



Fig. 13 – Overturned tractor after an 8.42 km h^{-1} rollover test.

directions (F_x and F_y). The peak strains obtained for S_1 and S_2 single gauges were 550 and 801.1 με, respectively. There were residual strains at the end of the test, since the tractor was still overturned and was loaded when the data acquisition was stopped. The corresponding impact load values generated on the anchor calculated from the measured strains by use of Eqs. (2)–(10) are given in Fig. 10.

The force normal to the diameter of the anchor (*y* direction) was found to be 55.18 kN whereas the one in the *x* direction, the travelling direction of the tractor, was 1.3 kN. The impact force measured in the *y* direction was found to be considerably higher which is consistent with the acceleration results obtain in the same direction. Although the force in the *z* direction was not measured accurately it could be estimated from Fig. 10 to be approximately 45 kN.

The strain *versus* time values for the ROPS, which were measured by rosette gauges, are given in Fig. 11. By use of strain values measured during the field upset test, the von Misses stress was calculated by use of Glyphworks software (nCode, USA) and the obtained stress values are given in Fig. 12.

Fig. 13 shows the overturned tractor. The plastic deformation can be easily seen in this figure. This deformation occurred due to the high acceleration of the tractor during rollover and the nature of the anchors. Because of the anchoring effect of the system, the movement of the tractor in the z direction was restricted and this led to an increase of force in the z direction. After completion of the test, this plastic deformation was measured as 270 mm. Even though the anchor was permanently deformed, there was no infringement into the clearance zone, which is due to the large safety zone of the anchor, and the bonnet of the tractor not coming into contact with the ground.

4. Conclusions

The anchor mechanism is a new attachment for the ROPS; therefore, current OECD codes do not completely cover the test procedures for this system. However, the stress generated on the pins can be determined by use of the static side-loading test. After the test, no failure was observed on the anchor mechanism, ROPS, joints and latch pins. When the simulated ground plane was considered for the static side-loading test, ROPS passed this cycle in limits but the anchor system provided a larger safety area. In the field upset test, the anchor was buckled, but there was no infringement into the clearance zone.

Acknowledgments

This research was funded by TUBITAK, Turk Traktor and Ziraat Makineleri A.S. The authors would like to thank TUBITAK, Turk Traktor and Ziraat Makineleri A.S and Ministry of Agriculture and Rural Affairs, Directorate of Agricultural Equipment and Machinery Test Centre, for their support.

REFERENCES

ASAE J2194 (2002). Roll-Over Protective Structures (ROPS) for Wheeled Agricultural Tractors. American Society of Agricultural Engineers, St Joseph, MI, USA

Day L; Scott M; Williams R; Rechnitzer G; Walsh P; Boyle S (2005). Development of the safe tractor assessment rating system. Journal of Agricultural Safety and Health, **11**(3), 353–364

Etherton J T; Cutlip R G; Haris J R; Ronaghi M; Means K H; Gillispe A (2002). Static load test performance of a telescoping structure for an automatically deployable ROPS. Journal of Agricultural Safety and Health, **8**(1), 119–126

Liu J; Ayers P D (1998). Application of a tractor stability index for protective structure deployment. Journal of Agricultural Safety and Health Special Issue(1), 171–181

Murphy D J; Sommer H J (2004). Display of stability data for safe tractor operation. Northeast Center for Agricultural Safety and Health Annual Report Summary Fiscal Year, New York, USA

Myers M L (2000). Prevention effectiveness of rollover protective structures, part I: Strategy evolution. Journal of Agricultural Safety and Health, **6**(1), 29–40

OECD (2007). Standard Codes for the Official Testing of Protective Structures Mounted on Agricultural and Forestry Tractors. Organisation for Economic Co-operation and Development, Paris, France

OECD Code 6 (2007). Standard Code for the Official Testing of front Mounted Roll-over Protective Structures on Narrow-track Wheeled Agricultural and Forestry Tractors. Organisation for Economic Co-operation and Development, Paris, France

Silleli H; Dayıoğlu M A; Gültekin A; Ekmekçi K; Yıldız M A; Akay E; Saranlı G (2007). Anchor mechanism to increase the operator clearance zone on narrow-track wheeled agricultural tractor: prototype and first tests. Biosystems Engineering, **97**(2), 153–161

Spencer H B; Owen G M; Glasbey C A (1985). On site measurement of stability of agricultural machines. Journal of Agricultural Engineering Research, **1**(31), 81–91